



Cite this: *Environ. Sci.: Nano*, 2025, 12, 5242

Characterizing nanoplastic suspensions of increasing complexity: inter-laboratory comparison of size measurements using dynamic light scattering

Korinna Altmann, ^{*,a} Raquel Portela, ^{*,b} Francesco Barbero, ^c Esther Breuninger, ^d Laura Maria Azzurra Camassa, ^e Tanja Cirkovic Velickovic, ^f Costas Charitidis, ^g Anna Costa, ^h Marta Fadda, ⁱ Petra Fengler, ^a Ivana Fenoglio, ^c Andrea M. Giovannozzi, ⁱ Øyvind Pernell Haugen, ^e Panagiotis Kainourgios, ^g Frank von der Kammer, ^d Markus J. Kirchner, ^{*,k} Madeleine Lomax-Vogt, ^d Tamara Lujic, ^f Frank Milczewski, ^a Mhamad Aly Moussawi, ^l Simona Ortelli, ^h Tatjana N. Parac-Vogt, ^l Annegret Potthoff, ^m Julian J. Jimenez Reinosa, ⁿ Sophie Röschter, ^m Alessio Sacco, ⁱ Lukas Wimmer, ^o Ilaria Zanoni ^h and Lea Ann Dailey ^o

Understanding the potential human health risks associated with micro- and nanoplastic exposure is currently a priority research area. Nanoplastic toxicity studies are complicated by the lack of available, well-characterized test and reference materials. Further, many nanoplastic test materials are inherently more polydisperse and heterogenous in shape compared to polystyrene beads, making accurate and representative size distribution measurements particularly challenging. The aim of this study was to conduct an inter-laboratory comparison of dynamic light scattering measurements, the most commonly used particle sizing method for nanomaterials. Using a published standard operating procedure, size measurements in water and a standardized cell culture medium (CCM) were generated for spherical, carboxy-functionalized polystyrene nanoparticles (PS-COOH; 50 nm; benchmark material), and for increasingly complex in-house produced spherical poly(ethylene terephthalate) (nanoPET) and irregular-

Received 16th July 2025,
Accepted 19th September 2025

DOI: 10.1039/d5en00645g

rsc.li/es-nano

Environmental significance

Nanoplastic test materials with increased complexity regarding shape, surface chemistry and polydispersity are developed to mimic environmental nanoplastics. These materials are used to study eco-corona formation, biodistribution, and toxicity. Particle size is a key parameter and dynamic light scattering (DLS) is widely used for size analysis. Nanoplastic complexity is challenging for DLS, which calculates size based on the assumption of monodisperse, spherical particles. To evaluate how nanoplastic complexity influences DLS measurements, an inter-laboratory comparison was performed. Nanosized PET (spherical, polydisperse) and nanosized PP (irregular, polydisperse) showed a similar variability for measurements in water and cell culture medium compared to spherical monodisperse polystyrene beads. We conclude that nanoplastic complexity does not increase DLS variability if validated protocols are used.

^a Bundesanstalt für Materialforschung und -prüfung (BAM), Unter den Eichen 87, 12205 Berlin, Germany. E-mail: korinna.altmann@bam.de

^b Instituto de Catalisis y Petroleoquímica (ICP), Materials Science Institute of Madrid (CSIC), -C/Marie Curie 2, Madrid, 28049, Spain. E-mail: raquel.portela@csic.es

^c Department of Chemistry, University of Torino (UNITO), Torino, Italy

^d Department of Environmental Geosciences (EDGE), University of Vienna, Josef-Holaubek-Platz 2, 1090 Vienna, Austria

^e Norwegian Institute of Occupational Health (STAMI), 0363 Oslo, Norway

^f University of Belgrade Faculty of Chemistry (UBFC), Belgrade, Serbia

^g National and Technical University of Athens (NTUA), Athens, Greece

^h National Research Council of Italy - Institute of Science, Technology and Sustainability for Ceramics (CNR-ISSMC), Via Granarolo 64, 48018 Faenza, Italy, Via Granarolo 64, 48018 Faenza (RA), Italy

ⁱ Quantum Metrology and Nano Technologies Division, Istituto Nazionale di Ricerca Metrologica (INRiM), Strada delle Cacce 91, 10135, Torino, Italy

^j University of Bayreuth, Animal Ecology I, Bayreuth Center of Ecology and Environmental Research (BayCEER), Universitätsstr. 30, 95447 Bayreuth, Germany

^k Department of Chemical and Product Safety, German Federal Institute for Risk Assessment (BfR), Max-Dohrn-Str. 8-10, 10589 Berlin, Germany

^l Department of Chemistry, KU Leuven, Celestijnenlaan 200F, 3001 Leuven, Belgium

^m Fraunhofer Institute for Ceramic Technologies and Systems (IKTS), Dresden, Germany

ⁿ Materials Science Institute of Madrid (CSIC), Instituto de Ceramica y Vidrio (ICV), C/Kelsen, Madrid, 28049, Spain

^o Department of Pharmaceutical Sciences, University of Vienna, Josef-Holaubek-Platz 2, 1090 Vienna, Austria. E-mail: leaann.dailey@univie.ac.at



shaped polypropylene (nanoPP) test materials. The weighted mean of hydrodynamic diameters of PS-COOH dispersed in water (55 ± 5 nm) showed moderate variation between labs (coefficient of variation, CV = 8.2%) and were similar to literature reports. Measurements of nanoPET (82 ± 6 nm) and nanoPP (182 ± 12 nm) in water exhibited similar CV values (nanoPET: 7.3% and nanoPP; 6.8%). Dispersion of PS-COOH and nanoPET in CCM increased the CV to 15.1 and 14.2%, respectively, which is lower than literature reports (CV = 30%). We conclude with a series of practical recommendations for robust size measurements of nanoplastics in both water and complex media highlighting that strict adherence to a standard operating procedure is required to prevent particle agglomeration in CCM.

1. Introduction

Understanding the potential human health risks associated with micro- and nanoplastic (NP < 1 μm)¹ exposure is currently a priority research area. Particularly, exposure to nanosized plastic materials, which may be intentionally produced for industrial/consumer applications (primary nanoplastic, increasingly regulated)^{2,3} or occur in the environment/consumer products as a result of microplastic breakdown (secondary nanoplastics)^{2,4} is of high concern. Nanoplastics are especially relevant since smaller particulates may be able to access cellular compartments or cross mucosal barriers to a greater extent than larger plastics.⁵ Nanoplastic *in vitro* toxicity studies are complicated, among other reasons, by the lack of available, well-characterized materials.^{6–8} Since nanoplastics developed for research purposes should have characteristics reflective of environmentally relevant nanoplastics, the materials under current development are inherently more polydisperse and heterogenous in shape compared to spherical, monodisperse polystyrene (PS) beads. They can exhibit a different surface charge and variable hydrophobicity making their homogenous dispersibility challenging, particularly in complex media.⁹ This is especially true for materials developed to mimic nanoplastics which have undergone environmental weathering.¹⁰

A second challenge is that model nanoplastics are required for different intended uses, the two most common being: 1) for the calibration of analytical instruments and 2) for testing the behavior and effects of nanoplastics in both an environmental and physiological context.^{11,12} While ideally the nanoplastics themselves should be identical in all applications, the nanoplastic products developed, which includes the choice of packaging (single unit or multi-unit containers), the concentrations provided, the presence of stabilizing additives, as well as the scope of testing and certification, will be very different depending on application. For example, a nanoplastic product developed as a standard for instrument calibration is typically provided at a concentration optimized for the instrument calibration process. Multiple handling steps, such as dilutions, are avoided to reduce sources of error. Additives, such as suspension stabilizers or preservatives, are acceptable if they do not influence the measurement. These products must also be rigorously tested for homogeneity and stability with respect to a specific property, in order to

achieve reference material status (Table 1).^{11,13–15} In contrast, nanoplastic products used for toxicology studies or to assess environmental disposition are ideally provided in concentrated form to allow for dosing flexibility. This necessitates additional handling steps, such as dilutions. Additives are frequently undesired, as they can cause artefacts in different assays. The suite of characterization methods required for these applications are typically quite different to those required for reference materials, often including detailed characterization of surface chemistry, product sterility, and/or endotoxin content.^{11,12} Based on these distinctions, such nanoplastic products are mainly categorized as research grade test materials (Table 1).

Since new nanoplastic materials are becoming increasingly available to the research community for a variety of applications,^{6,8,10,12,17–19} questions have been raised as to the accuracy and reproducibility of size measurements using dynamic light scattering (DLS) for these more irregular, polydisperse materials.²⁰ To evaluate the precision and accuracy of DLS measurements on such nanoplastic dispersions, an inter-laboratory comparison (ILC) focused on nanoplastics was conducted. Two types of nanoplastic product formats were examined. The first was a research grade test material comprised of nanosized polyethylene terephthalate (nanoPET), which was provided in concentrated form requiring multiple dilution steps. Since the nanoPET product was designed for use in *in vitro* toxicity assays, an understanding of colloidal behavior and size stability in cell culture medium (CCM) was also investigated.^{9,21–24} The second product comprised a nanosized polypropylene (nanoPP) dispersion. This product was designed for instrument calibration, in particular for size measurements using DLS, with the aim of applying for reference material status following completion of homogeneity and stability testing.

Several key reports on the evaluation of DLS measurements for nanoplastics (in particular polystyrene) in both simple and complex media have been published.^{21,25–27} Notably, Langevin *et al.* (2018) conducted an ILC investigating the accuracy and reproducibility of nanoparticle size measurements in biological media for two commonly used particle sizing methods, *i.e.* DLS and differential centrifugal sedimentation.²⁶ They recruited 40 labs to participate, although not all labs provided data in all rounds. They measured three types of well-characterized materials: 1) near-spherical silica nanoparticles (reported diameters: 19 nm and 100 nm), 2) spherical, carboxy-modified polystyrene



Table 1 National Institute of Standards and Technology (NIST) and International Organization for Standardization (ISO) categories and definitions of materials^{13–16}

| Category | Definition |
|-----------------------------------|---|
| Research grade test material | Exploratory materials developed for current research needs, which are subject to continuous stability measurements. The extent of characterization depends on the needs of the user community and is therefore not standardized |
| Reference material | A material, homogeneous and stable with respect to one or more specified property values, which has been established to be for its intended use in a measurement process |
| Certified reference material | A material characterized by a metrologically valid procedure for one or more specified properties, accompanied by a reference material certificate that provides the value of the specified property, its associated uncertainty, and a statement of metrological traceability |
| NIST standard reference material® | A certified reference material issued by NIST that also meets additional NIST-specific certification criteria and is issued with a certificate or certificate of analysis that reports the results of its characterizations and provides information regarding the appropriate use(s) of the material |

nanoparticles (PS-COOH; reported diameter: 50 nm) and 3) spherical, amine-modified polystyrene nanoparticles (reported diameter: 50 nm). All materials were measured first in water, then in CCM.

In the first ILC round, each laboratory used their in-house established procedures. Following this, a harmonized standard operating procedure (SOP) was developed by four expert laboratories and tested for robustness by eleven independent users in a second round (published in full in the SI). A bespoke SOP was developed for measurements in CCM and was tested by eight participating laboratories. The authors concluded that well-established and fit-for-purpose SOPs are indispensable for obtaining reliable and comparable particle size data, especially when measuring in complex media. Importantly, the SOPs must be optimized with respect to the intended measurement system (*e.g.* particle size technique, type of dispersant) and must be sufficiently detailed to avoid ambiguity.

In subsequent studies, Takahashi *et al.* (2019) and Coones *et al.* (2025) addressed the question of how to relate particle sizes measured using a fixed-angle DLS instrument with those measured using a multi-angle DLS.^{25,27} The focus of these more technical studies was to establish the functional dependence of the measured particle size on the scattering angle and particle concentration. However, since the aims and scope of the Langevin *et al.* (2018) study more closely matched the interests of the nanoplastic research community, we chose to adopt their study design and use their SOPs for the current study.

To enable direct comparison of our results to published data, we chose to include the same spherical, monodisperse PS-COOH nanoparticles (nominal 50 nm diameter) as a benchmark material. Additionally, we evaluated two nanoplastic test materials (Fig. 1) produced by projects of the CUSP cluster funded by the Horizon2020 program of the European Commission (<https://cusp-research.eu/>) and the Metrology Partnership project 21GRD07 PlasticTrace (<https://plastictrace.eu/>). NanoPET test materials were produced *via* a bottom-up anti-solvent precipitation method with a final concentration of ~ 6 mg mL⁻¹. The preparation

via precipitation yielded particles with a spherical morphology, moderate polydispersity and an electronegative surface charge with a zeta potential of -42 ± 2 mV (pH 4.75; MilliQ water, conductivity: 0.009 ± 0.0005 mS cm⁻¹). NanoPP reference materials were prepared *via* a top-down approach using milling in chilled acetone to produce submicron-sized fragments at a more dilute concentration (0.04 mg mL⁻¹). Since nanoPP materials were produced *via* mechanical breakdown,⁶ the particles exhibited an irregular morphology (Fig. 1). In MilliQ water (pH 4.75; conductivity: 0.009 ± 0.0005 mS cm⁻¹), the nanoPP also displayed an electronegative surface charge with a zeta potential of -43 ± 2 mV.

Since PS-COOH and nanoPET test materials were designed for multiple applications and therefore provided as highly concentrated suspensions, both systems had to be diluted prior to DLS measurement to a concentration of 0.1 mg mL⁻¹. NanoPP test materials, in contrast, were designed to be used as reference materials for instrument calibration purposes only. As stated above, it is advantageous in such applications to provide the material in a ready-to-use form which negates the need for additional handling steps. Thus, the nanoPP provided in this study had a low concentration of 0.04 mg mL⁻¹ in water. Since it was not possible to dilute this material with CCM and remain in a measurable concentration range, nanoPP was only tested in water during this study.

Firstly, we hypothesized that increased nanoplastic material complexity, especially regarding shape and polydispersity, would result in higher measurement variability when measuring in water. Secondly, it is known that dilution into complex media with high ionic strength, such as serum-supplemented CCM, may influence the particle size distribution determined by DLS⁹ and increase variability. Therefore, a second aim of this study was to establish simple quality criteria for DLS measurements of more complex nanoplastic samples, which can be easily adopted and understood by user groups without expert-level knowledge of DLS. Since particle size and size distribution are crucial parameters in toxicity studies, this ILC provides recommendations to harmonize size



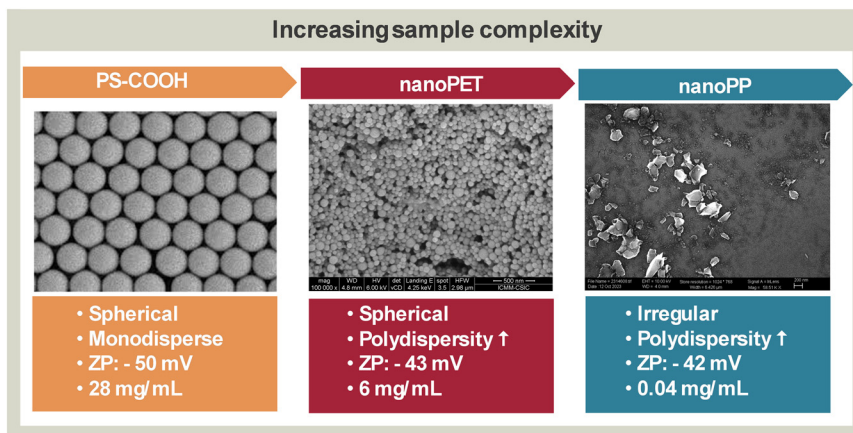


Fig. 1 Description and representative scanning electron micrograph (SEM) images of the three test materials used in the study: PS-COOH, nanoPET and nanoPP. Note: The image of the polystyrene beads is a representative image from the manufacturer website²⁸ and is not provided at scale.

characterization measurements across the nanoplastic research community.

2. Materials and methods

2.1. Materials

Aqueous dispersions of polystyrene beads with carboxyl surface functionalization (PS-COOH) were purchased from Polysciences, Inc. (catalog number 15913-10). Two lots were used in the study: 1) lot#A844160 used in labs #3, 8, 10, and 11 contains 2.8% solids (w/v) with a reported diameter of 49 nm and a coefficient of variation (CV) of 14%; 2) lot #A844160 used in labs #1, 11 and 15 contains 2.7% solids with a reported diameter of 49 nm and a CV of 14%. Polypropylene granules were kindly provided by PlasticsEurope (Moplen RP320M, LyondellBasell). NanoPET was produced from RAMAPET N180 granules. MilliQ water had electrical resistivity <math><18.2\text{ M}\Omega\text{ cm}</math>. Complete cell culture medium (CCM) typically contained modified Eagle medium (MEM), Glutamax provided by different suppliers (Gibco: #41090-028; VWR: #VWRMS024F; Corning: #10-009-CV); 10% fetal bovine serum (FBS; non-heat inactivated from Gibco: #P220303; Avantor; Biowest: #1860; Sigma: # 1670543; Capricorn Scientific: LOT CP20-3579; Biological Industries: LOT 1348500; ATCC: 80715235) and 100 U mL⁻¹ penicillin/100 µg mL⁻¹ streptomycin (Invitrogen:15070063). Labs 8, 12, 13, 14 substituted Dulbecco's modified Eagle medium (DMEM; Gibco: 2858875) for MEM.

2.2. Production of nanoPET

In a fume hood, following the method described by,²⁹ 1 g PET (pellets) was dissolved in 100 mL hexafluoroisopropanol (HFIP) at room temperature and injected at controlled velocity into 1 L of ice-cooled, sterile MilliQ water. Excess water and HFIP were removed *via* rotary evaporation (-70 °C, -86 kPa for a minimum of 2 h) until a desired final concentration of ~6 mg mL⁻¹ was achieved. The internal code was PET_c003.

2.3. Production of nanoPP

NanoPP test materials were prepared according to a method described by Hildenbrandt *et al.*⁶ Briefly, polypropylene granules (6.25 g) were added to a 400 mL glass beaker containing acetone (250 mL) chilled to 0 °C. The polymer granules were milled with an IKA T 18 digital ULTRA-TURRAX for 10 min at a rotation speed of 18 000 rpm. The suspension was then filtered using a folded filter to remove the larger aggregates. Acetone in the filtrate was evaporated until *ca.* 10% of the liquid remained, then MilliQ water (250 mL) was added to the mixture, the remaining acetone was removed with a rotary evaporator and the suspension filtered using a folded filter. The nanoPP is provided as a MilliQ water suspension without any further stabilizing additives and a concentration of 0.04 mg mL⁻¹.

2.4. Scanning electron microscopy and size analysis

NanoPET and nanoPP suspensions were dropcast onto a glass slide, fixed onto a sample holder with double-sided conductive adhesive tape and dried overnight. On the following day, the samples were gold-sputtered and imaged with an EVO MA 10 (Zeiss, Oberkochen, Germany) using secondary electron contrast mode with voltages of 10 kV. Particle size distributions were generated from the SEM images by measuring the Feret diameter of the spherical nanoPET particles ($n = 100$) and the minimum and maximum Feret diameter for the irregular nanoPP particles ($n = 84$) following recommendations provided by Bresch *et al.*³⁰ Aspect ratios were calculated as the ratio between the maximum:minimum Feret diameter. The PS-COOH distribution was calculated from the reported diameter and CV% provided by the manufacturer, while the image is provided by the manufacturer.

2.5. Preparation of dispersions in water and CCM

PS-COOH and nanoPET were assessed by preparing three separate dilutions (three experimental replicates) and



measuring each sample three times (three technical replicates). MilliQ water and CCM were filtered (0.2 μm pore diameter) prior to use to remove ambient particulates. Stock suspensions (1 mg mL^{-1}) of PS-COOH and nanoPET were prepared with the filtered MilliQ water and mixed for 30 s using a benchtop vortex at full speed. Immediately, 100 μL stock suspension was added to either 900 μL water or CCM (final sample concentration: 0.1 mg mL^{-1}) in separate sterile 1.5 mL polypropylene tubes and further vortexed for a further 30 sec at full speed. Samples were then measured immediately. It should be noted that each lab sourced their own CCM components, resulting in slight variations between the providers of medium and FBS (see section 2.1). Labs 8, 12, 13 and 14 also substituted DMEM for MEM in their experiments.

The nanoPP samples were provided as an aqueous dispersion at a concentration of 0.04 mg mL^{-1} and were therefore measured as received without dilution. Prior to measurement, samples were briefly vortexed for 30 s at full speed and measured immediately ($n = 3$ separate aliquots with $n = 3$ technical replicates each).

2.6. DLS measurements

Variability due to handling and dilution was assessed by preparing three separate sample dilutions and measuring each sample three times ($n = 9$ total). Within one measurement sequence, the DLS instrument performs 3–10 measurements for each sample, which correspond to one technical replicate. The DLS instruments listed in Table 2 were used in the study.

Quartz or high-quality optical glass cuvettes were recommended, but good quality plastic cuvettes were also included in the study parameters. All cuvettes, but in particular the more scratch-prone plastic cuvettes, were routinely inspected prior to use and discarded if surface scratches or defects were visible. Clean cuvettes were pre-rinsed with filtered MilliQ water at least three times prior to

sample loading (preferably in a high efficiency particulate air-filtered clean bench if available). The required volume of NP dispersion was filled into the DLS cuvette using the minimum volume necessary to ensure that the liquid level was at least 2 mm above the entrance height of the laser beam. Overfilling was avoided to prevent thermal gradients that adversely impact measurement accuracy. Cuvettes were visually inspected to ensure that air bubbles were not present within the optical window area prior to insertion into the instrument. Measurements were conducted at temperatures close to ambient room temperature, ideally between 23–25 $^{\circ}\text{C}$. Diluent viscosity values and refractive indices for all materials can be found in Table 3.

The Z-average (Z-Ave) value of the nine DLS measurements is derived from the cumulants approach for calculating the average size of a distribution of particles based on analysis of the linear form of the measured correlogram (scattered light intensity-weighted harmonic mean hydrodynamic diameter). The analysis assumes that the particles belong to a single population which follows a Gaussian distribution. The polydispersity index (PDI) is the relative variance of the hypothetical Gaussian distribution.^{32–34} Representative examples of particle size distribution curves and fitted correlograms are provided in the (SI) Fig. S1 and S2. No evidence of particle sedimentation or flotation was reported during the time course of all measurements. Files with all raw data are available in Zenodo: <https://doi.org/10.5281/zenodo.17105630>.

2.7. Statistical analysis

The DLS results were analyzed using the arithmetic mean (x_i) and standard deviation (SD_i) for individual datasets from each laboratory. Samples with polymodal size distributions, indicative of particle agglomeration, were excluded from the statistical analysis (example SI Fig. S3). Global means from the ILC were calculated using both a weighted and non-weighted approach. Non-weighted averages represent the

Table 2 Instruments used in the ILC study, including information on the detection angle and operator experience level in years

| Lab | Instrument | Detection angle $^{\circ}$ | Operator experience (years) |
|-----|---|--|-----------------------------|
| 1 | NanoZS (Malvern Panalytical) | 173 $^{\circ}$ backscatter | 2 |
| 2 | Nano ZSP (Malvern Panalytical) | 173 $^{\circ}$ backscatter | 3 |
| 3 | Zetasizer Pro Blue Light Scattering System (ZSU3200; Malvern Panalytical) | Not provided | 4 |
| 4 | ZetaSizer Ultra (Malvern Panalytical) | 173 $^{\circ}$ backscatter | 7 |
| 5 | NanoZS ZEN 3600 (Malvern Panalytical) | 173 $^{\circ}$ backscatter | 10 |
| 6 | NanoZS (Malvern Panalytical) | 173 $^{\circ}$ backscatter | 2 |
| 7 | NanoZSP (Malvern Panalytical) | 173 $^{\circ}$ backscatter | 10 |
| 8 | NanoZS (Malvern Panalytical) | 173 $^{\circ}$ backscatter | 4 |
| 9 | NanoZS ZEN 3600 (Malvern Panalytical) | 173 $^{\circ}$ backscatter | 2 |
| 10 | NanoZS (Malvern Panalytical) | 173 $^{\circ}$ backscatter | >10 |
| 11 | NanoZS (Malvern Panalytical) | 173 $^{\circ}$ backscatter | >25 |
| 12 | NanoZS (Malvern Panalytical) | 173 $^{\circ}$ backscatter | 12 |
| 13 | NanoZS (Malvern Panalytical) | 173 $^{\circ}$ backscatter | 1 |
| 14 | Litesizer500 (Anton Paar) | 175 $^{\circ}$ backscatter | 1 |
| 15 | Litesizer500 (Anton Paar) | 90 $^{\circ}$ and 175 $^{\circ}$ backscatter | >10 |
| 16 | NanoPlus-3 (Micromeritics) | 160 $^{\circ}$ (automatic) | 1 |



Table 3 Values used for instrument settings. Viscosity values were taken from²⁶

| | Viscosity (mPa s) | Refractive index |
|---------------------|-------------------|--------------------|
| Water 23 °C | 0.932 | 1.330 ^a |
| Water 24 °C | 0.910 | |
| Water 25 °C | 0.890 | |
| Cell culture medium | 1.090 | 1.335 ^a |
| PS-COOH | — | 1.590 ^b |
| nanoPP | — | 1.490 ^b |
| nanoPET | — | 1.569 ^b |

^a Suitable for wavelengths between 488–750 nm within the temperature range of 20 °C to 25 °C. ^b Suitable for wavelengths between 400 nm – 2 μm within the temperature range of 20 °C to 25 °C.³¹

arithmetic mean (x_{nw}) and standard deviation (SD_{nw}) from the x_i values of all partners. The weighted mean (eqn (1)) was defined as:

$$x_w = \frac{\sum_{i=1}^n w_i x_i}{\sum_{i=1}^n w_i} \quad (1)$$

whereby, $w_i = 1/(SD_i)^2$ and x_i is the arithmetic mean for individual laboratory measurements. The weighted mean reduces the influence of data sets with high dispersion values on the final average value. It is considered to be more robust compared to the non-weighted arithmetic mean because the contribution of highly scattered data is reduced. The SD and coefficients of variation (CV) were calculated using both non-weighted and weighted means for comparison. The CV is defined as the ratio between the SD and the corresponding mean multiplied by 100.

According to ISO/IEC 17043:2010,³⁵ the measurements of ILC contributor laboratories are acceptable if $x_i \pm SD_i$ falls within the range of $x_w \pm 2SD_w$. Thus, all black lines in figures represent x_w while dashed lines represent $\pm 2SD_w$ and define the consensus interval in which the results are expected to fall assuming a confidence level of 95%.

3. Results and discussion

3.1. Size analysis from SEM images

All analytical techniques for measuring particle size have inherent strengths and weaknesses, depending on the principle underlying the measurement. They can also provide different types of information, such as size metrics (*i.e.* equivalent diameters) or size and shape metrics.^{35,36} It is therefore recommended that a combination of direct sizing methods (image-derived) and indirect methods (including but not limited to small angle X-ray scattering, DLS, laser diffraction, nanoparticle tracking analysis, analytical centrifugation, field flow fractionation combined with light scattering methods, acoustic spectroscopy, tunable resistive pulse sensing) is performed.^{35,36} Manufacturers of nanoplastic test materials typically have access to a wider

range of these analytical techniques and will employ multiple sizing methods during the material characterization phase. Material users, in contrast, typically only have access to a limited range of sizing equipment and rely heavily on DLS measurements for size characterization. This is why DLS benchmarking studies between material manufacturers and users is highly valuable.

SEM images of nanoPET and nanoPP (Fig. 1) were used to assess the Feret diameter distributions and particle aspect ratios of the nanoPET and nanoPP samples (Fig. 2). Size distribution data of the PS-COOH samples was provided in the material data sheet of the commercial product. The analysis verifies the hypothesis that particle complexity increases in terms of polydispersity and shape irregularity over the series of nanoplastics tested (complexity: PS-COOH < nanoPET < nanoPP).

3.2. DLS evaluation of PS-COOH and benchmarking to the literature

3.2.1. Measurement of PS-COOH in water. Eleven labs independently acquired the PS-COOH benchmark material and provided intensity-based Z-average (Z-Ave) measurements in water. Ten of eleven lab datasets ($x_i \pm 1SD_i$) were within the consensus range of $x_w \pm 2SD_w$ (Fig. 3). Both the weighted and non-weighted mean hydrodynamic diameters (55 and 57 nm, respectively) were similar to the first round of the ILC reported by Langevin *et al.* (2018) but larger than the sizes measured in the second round (Table 4), where the same SOP was used.²⁶ As expected for the PS-COOH, the PDI values were close to 0.05 (Fig. 3) indicating a uniform monodisperse sample in all cases except for two labs. According to guidelines, the PDI is a dimensionless and scaled value, calculated from a two-parameter fit to the correlation data (the cumulants analysis). PDI values can be interpreted as follows: <0.05 = uniform monodisperse, 0.05–0.1 = narrow monodisperse, 0.1–0.4 = moderately polydisperse, 0.4–0.7 = broadly polydisperse, and >0.7 = too polydisperse for DLS measurement.^{32,36}

3.2.2. Measurement of PS-COOH in CCM. Eight of the eleven labs provided measurements of PS-COOH in CCM; however, three of the eight datasets reported sample agglomeration (example SI Fig. S3) and were excluded from the statistical analysis. Variations in sample handling were identified as the cause of agglomeration and are discussed in detail in sections 3.5 and 3.6. The remaining five monomodal datasets (example SI Fig. S2) were within the consensus range (Fig. 3). The global weighted mean x_w increased from 55 nm in water to 60 nm in CCM, with a low CV_w of 5.3%, which was substantially lower than the 30% reported by Langevin *et al.*, 2018. This may be influenced by the low sample number in the current study as well as the exclusion of agglomerated samples. The PDI of monomodal PS-COOH dispersions in CCM clustered around ~0.2 (moderately polydisperse; Fig. 3). Interestingly, the CCM composition (MEM *vs.* DMEM) did not appear to influence the size and



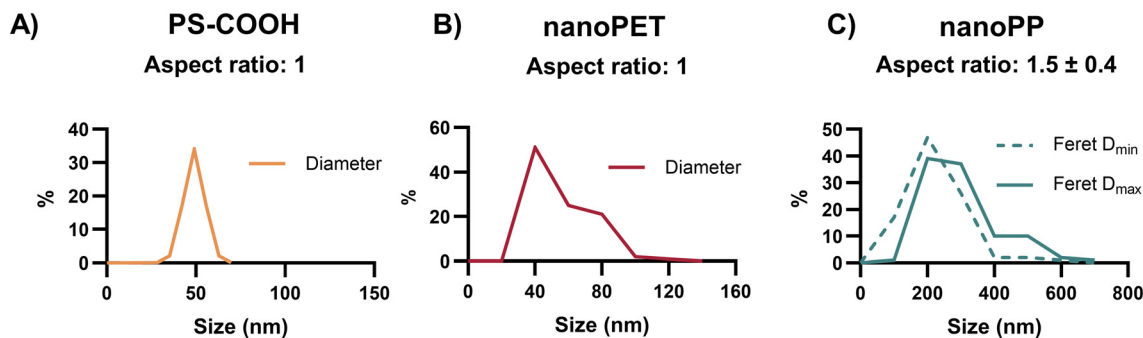


Fig. 2 SEM-derived particle size distributions were generated from the Feret diameters of the spherical nanoPET particles (B; $n = 100$) and the minimum and maximum Feret diameters for the irregular nanoPP particles (C; $n = 84$).³⁰ The PS-COOH distribution (A) was calculated from the reported diameter and CV% provided by the manufacturer.

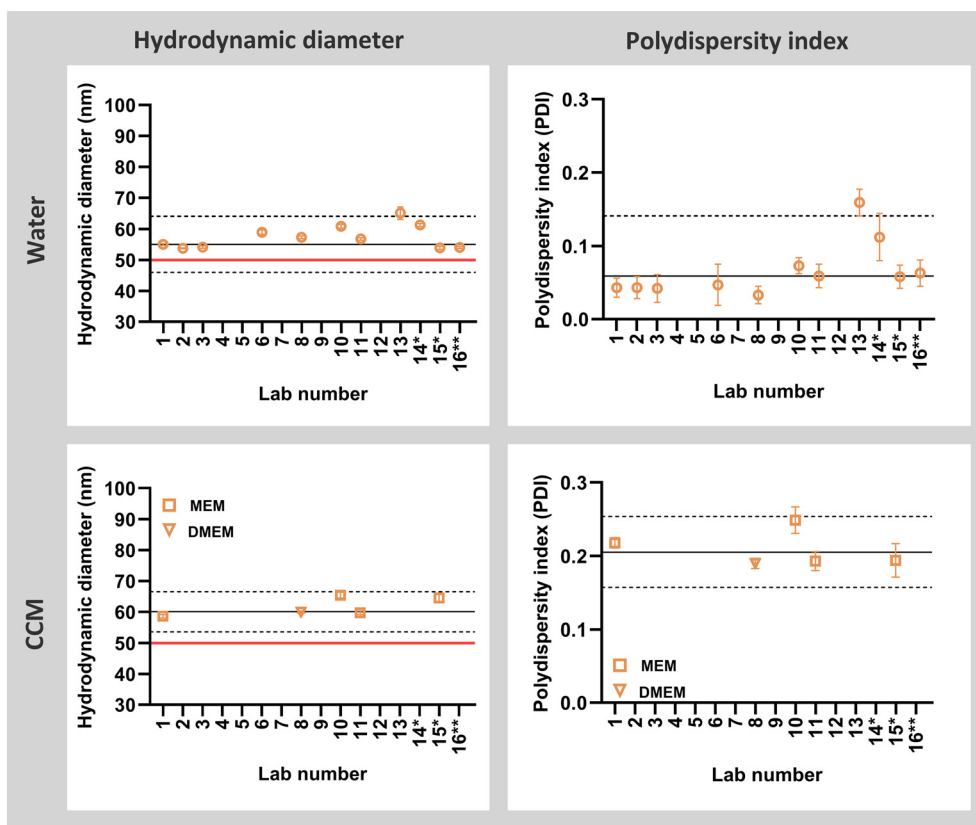


Fig. 3 Scattered light intensity-based harmonic mean hydrodynamic diameter (Z-Ave, left) and PDI values (right). PS-COOH measurements in water (top) are compared to CCM (bottom). Values for each lab depict the $x_i \pm 1SD_i$ ($n = 9$). Solid red lines depict the reported diameter provided by the manufacturer, black lines show the weighted global mean x_w , and dashed lines correspond to $\pm 2SD_w$. Lab numbers without asterisks denote Malvern Pananalytic devices, *Anton Paar, **MicroMeritics.

PDI, although the limited sample number prevents conclusive interpretations. Overall, results from this small-scale benchmarking study showed that measurements of uniform, monodisperse PS-COOH test materials in water were in the expected size range with a low variability between labs. Measurements in CCM were generally comparable to the results from Langevin *et al.*, 2018. This observation reinforces previous literature discussions which highlight that the dispersion of nanomaterials in complex media can negatively impact colloidal stability and therefore requires

strict adherence to validated SOPs for robust DLS size measurements.^{9,26}

3.3. DLS evaluation of nanoPET and nanoPP

3.3.1. Measurement of nanoPET in water. All sixteen labs had access to the same batches of nanoPET and nanoPP. As seen in the SEM image in Fig. 1, the nanoPET preparation method produced nearly spherical particles with an expected size of ~ 80 nm and a narrow but not uniform distribution.



Table 4 Summary of statistical analysis of PS-COOH hydrodynamic diameter values following dispersion in water and CCM reported in the current study and by Langevin *et al.* (2018). The reported diameter from the manufacturer was 49 nm. Mean, SD and CV values were calculated from the non-weighted and weighted global means

| | | Water | | | CCM | |
|--------------------------|-----------------|----------------------------|--|--|----------------------------|--|
| | | Current study ^b | Langevin <i>et al.</i> ILC #1 ^a | Langevin <i>et al.</i> ILC #2 ^b | Current study ^b | Langevin <i>et al.</i> ILC #3 ^b |
| Non-weighted global mean | x_{nw} (nm) | 57 | n.d. | n.d. | 62 | n.d. |
| | $1SD_{nw}$ (nm) | 4 | n.d. | n.d. | 3 | n.d. |
| | CV_{nw} (%) | 6.4 | n.d. | n.d. | 4.7 | n.d. |
| Weighted global mean | x_w (nm) | 55 | 55 | 46 | 60 | 50 |
| | $1SD_w$ (nm) | 5 | 3 | 2 | 3 | 15 |
| | CV_w (%) | 8.2 | 5.5 | 4.4 | 5.3 | 30.0 |
| | n | 87 | 162 | 199 | 45 | 72 |

^a Denotes no common SOP. ^b Denotes use of the same SOP. n.d. = not determined.

When diluted in water to the test concentration (0.1 mg mL⁻¹), all size distribution curves were monomodal; however, two datasets were outside the consensus range (Fig. 4). The measurement variability was hypothesized to increase for nanoPET, due to the different production method (nanoprecipitation for nanoPET compared to emulsification polymerization for PS-COOH). However, the CV_w of nanoPET (7.3%; Table 5) was slightly lower than the corresponding value for PS-COOH (8.2%). The PDI values cluster around 0.1 (Fig. 4), indicating that the material is

on the border between narrowly monodisperse and moderately polydisperse.

3.3.2. Measurement of nanoPET in CCM. Nine datasets for measurements of nanoPET in CCM were submitted (Fig. 4). All datasets were monomodal except for labs #10 and 15, which reported particle size distribution curves containing a second minor peak at 5–10 nm (example SI Fig. S4), typical of proteins/protein aggregates in CCM.³⁷ The presence of this minor peak was sufficient to shift the Z-Ave values for these samples to lower diameters, compared to samples without

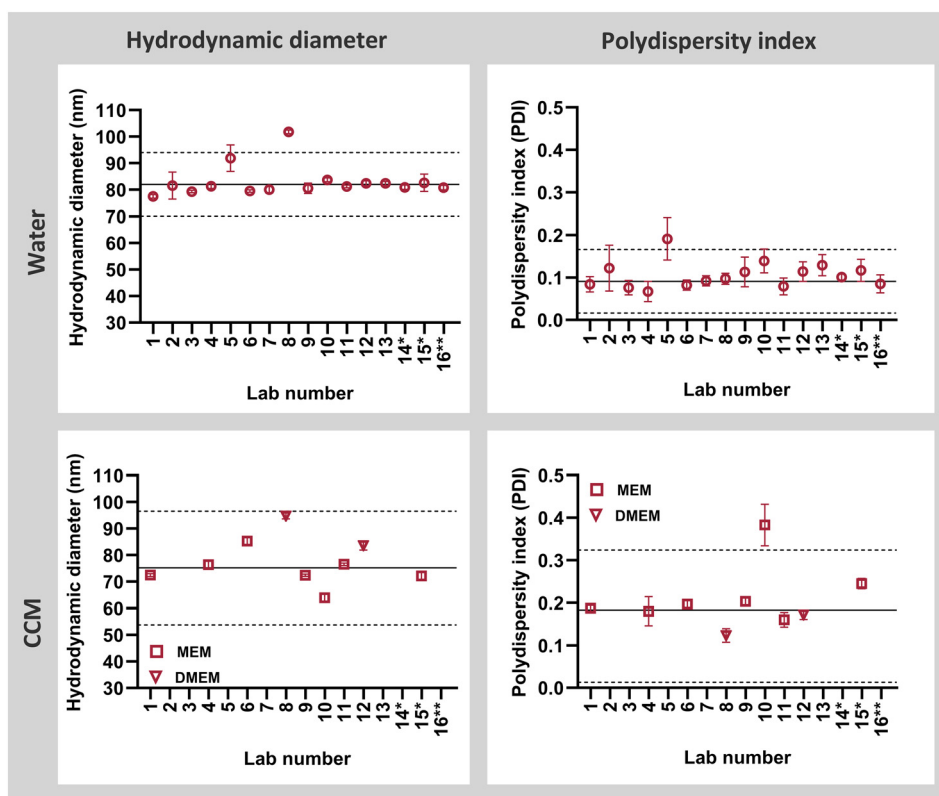


Fig. 4 Scattered light intensity-based harmonic mean hydrodynamic diameter (Z-Ave, left) and PDI values (right). nanoPET measurements in water (top) are compared to CCM (bottom). Values for each lab depict the $x_i \pm 1SD_i$ ($n = 9$). Black lines depict the weighted global mean x_w , and dashed lines correspond to $\pm 2SD_w$. Lab numbers without asterisks denote Malvern Panalytic devices, *Anton Paar, **MicroMeritics.



Table 5 Statistical analysis of the DLS data from the nanoPET and nanoPP test materials. Two analyses were performed for the nanoPET dispersion in CCM: #1 standard analysis with Z-Ave values and #2 alternative analysis with mode values from labs #10, and 15

| | | nanoPET (water) | nanoPET (CCM) #1 | nanoPET (CCM) #2 | nanoPP (water) |
|--------------------------|-----------------|-----------------|------------------|------------------|----------------|
| Non-weighted global mean | x_{nw} (nm) | 83 | 78 | 80 | 187 |
| | $1SD_{nw}$ (nm) | 6 | 9 | 8 | 13 |
| | CV_{nw} (%) | 7.6 | 11.2 | 9.5 | 7.1 |
| Weighted global mean | x_w (nm) | 82 | 75 | 75 | 182 |
| | $1SD_w$ (nm) | 6 | 11 | 12 | 12 |
| | CV_w (%) | 7.3 | 14.2 | 16.5 | 6.8 |
| | n | 132 | 81 | 65 | 138 |

the second peak (Fig. 4). This is a recognized phenomenon explored by Balog *et al.* (2015). To reduce the background signal arising from a biological matrix, they employed technique known as depolarized DLS, which may be useful for measuring certain types of nanomaterials which exhibit sufficient optical anisotropy.³⁷ Since this approach has not been explored for nanoplastics, we recommend a simpler solution. For example, in samples where a serum peak is present, it is possible to substitute the Z-Ave value with the mode of the highest intensity peak. This approach (example #2 in Table 5) reduces the differences between the global means measured in water and CCM and decreases the overall data variation. The PDI values range between 0.1–0.4 (Fig. 4), although it should be noted that labs reported serum peaks were included in the figure. Again, the CCM composition (MEM vs. DMEM) did not appear to influence the size and PDI, although the limited sample number requires further investigation.

3.3.3. Measurement of nanoPP in water. As seen in the SEM image in Fig. 1, the nanoPP preparation method produced irregular particles with an aspect ratio of ~ 1.5 , an expected size centered around 200 nm and a polydisperse distribution (Fig. 2). The top-down method of preparation, *i.e.*, wet-milling of larger plastics to smaller sizes, is often associated with low yields in the submicron size range and is the primary reason why this material is not provided as a

concentrated suspension like PS-COOH and nanoPET. Since this material is designed for use as a reference material for instrument calibration, the lower concentration (0.04 mg mL^{-1}) can have benefits since the product does not require additional handling steps like dilution. Datasets from two of sixteen labs were outside the consensus range (Fig. 5 and Table 5), but otherwise there was a relatively low variability with a CV of 6.8%. The PDI values of cluster around 0.1 (Fig. 5), indicating that the material is on the border between narrowly monodisperse and moderately polydisperse. This observation is of particular interest, since it demonstrates that nanoplastic dispersions with irregular shapes and a moderate aspect ratio, can still be measured with suitable reliability using DLS. However, it should be highlighted that despite their higher polydispersity and irregular shape, the nanoPP material is still a model nanoplastic and therefore exhibits a greater degree of homogeneity than nanoplastics extracted from the environment. DLS users should be aware that if environmentally derived nanoplastic samples show too high a polydispersity, DLS is likely not a suitable method for size characterization.

3.4. Colloidal stability of nanoplastics in water

Nanoplastic suspensions can be classified as colloidal dispersions, where the solid particles are typically in the size

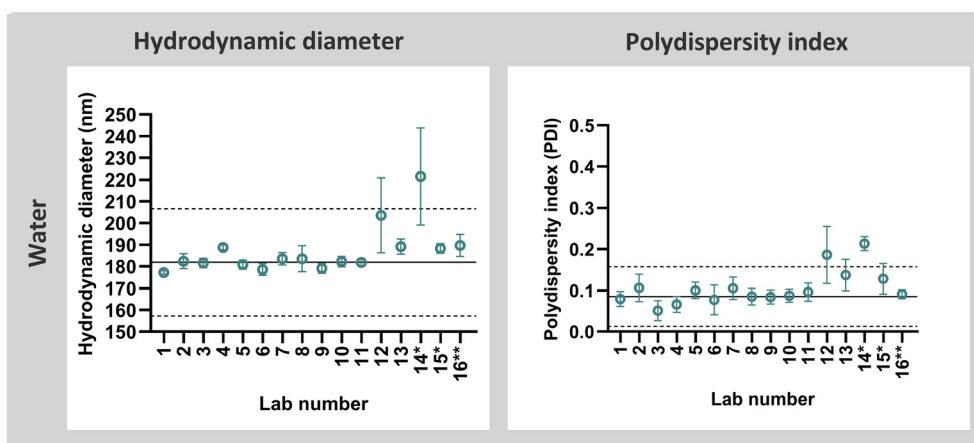


Fig. 5 Scattered light intensity-based harmonic mean hydrodynamic diameter (Z-Ave, left) and PDI values (right). nanoPP size measurements were performed with undiluted samples in water. Black lines depict the weighted global mean x_w , and dashed lines correspond to $\pm 2SD_w$. Values for each lab depict the $x_i \pm 1SD_i$ ($n = 9$). Lab numbers without asterisks denote Malvern Pananalytic devices, *Anton Paar, **MicroMeritics.



range of 10–1000. The colloidal stability of nanomaterials in a polar liquid such as water, is determined by the balance of attractive and repulsive forces between particles in the medium. Attractive forces include intermolecular and surface forces (e.g. van der Waals forces, hydrophobic interactions and structural forces such as depletion attraction). Van der Waals attraction, one of the most prevalent aggregation mechanisms, results from the interaction of induced, instantaneous, or permanent dipoles with opposite charge occurring on the nanomaterial surface. Van der Waals interactions are short-ranged and therefore require a close proximity of the two particle surfaces to form, which is why highly concentrated dispersions are more prone to agglomeration.⁹

The most important repulsion mechanisms include 1) charge repulsion (when the electrostatic charge of two neighboring particles are similar and repulse each other) and 2) steric repulsion (when two particles exhibit irregular surfaces that prevent close contact of particle surfaces thus reducing attractive forces). Since most nanomaterials carry some surface charge in aqueous environments due to the ionization/dissociation of surface groups, or the adsorption of charged molecules or ions to the particle surface, they show some form of charge repulsion. The true surface charge is not easy to measure and is therefore commonly approximated by measuring the zeta potential (ZP) value in a dilute salt solution (typically 10–15 mM sodium chloride). The ZP is the electrostatic potential of the particles measured at the shear plane, *i.e.* at the distance from the surface where ions are not bound to the particle. For more background information on the ZP, please refer to the following sources.^{38–41} Importantly, a highly positive or negative zeta potential (typically greater than ± 30 mV) indicates a sufficient charge repulsion for good colloidal stability in aqueous dispersants.⁴² Additives to dispersion media which alter the ion content (e.g. electrolytes) or pH (e.g. buffers) will alter the charge state of the particles (and the ZP value) with the possibility of charge neutralization, which can result in aggregation through a reduction in charge repulsion.⁹

When considering the chemical structure of the nanoplastics used in the current study, we would expect the ZP of the PS-COOH to be highly negative in a diluted salt solution with a neutral pH (Fig. 1), since the majority of the carboxyl groups at the surface will be deprotonated and carry an anionic charge. Contrary to expectations, the ZP of the nanoPET and nanoPP used here are also negative (Fig. 1), a phenomenon that has been reported for other micro- and nanoplastics.^{6,24} The observation of strongly electronegative ZP values measured for insoluble, hydrophobic micro- and nanoplastics dispersed at a physiological pH is a controversial topic in plastics research. Among the diverse explanations for the negative ZP of hydrophobic particles are the adsorption of anionic species such as hydroxyl⁴³ and bicarbonate ions⁴⁴ to the particle surface, interfacial polarization,⁴⁰ adsorption of

charge transfer between water molecules,⁴⁵ and surface-active charged impurities.^{46,47}

In addition to the mechanisms described above, we also hypothesize that the respective fabrication methods (nanoprecipitation and wet-crushing) may play a role in introducing charged functional groups (e.g. hydroxyl, carbonyl or carboxyl groups) to the nanoPET and nanoPP surface, improving their colloidal stability in aqueous media, even at higher concentrations.¹⁹ It is intriguing to observe that even minor differences in production procedures, such as the choice of solvents, can result in test materials with vastly different colloidal stability.¹⁹ For example, Wimmer *et al.* (2025), produced PET nanoplastics by dissolving PET in heated benzyl alcohol and precipitating into chilled ethanol. Dispersion of these PET nanoplastics was not possible in aqueous media without a surfactant stabilizer,¹² indicating a lack of surface charge necessary for colloidal stability. In contrast, the nanoPET studied here was dissolved at room temperature in HFIP and precipitated directly into water, forming nanoparticles with sufficient surface charge for colloidal stability at concentrations up to ~ 6 mg mL⁻¹. Similarly, Wimmer *et al.* (2025) prepared nanosized PP materials by dissolving PP in heated xylene and injecting it into chilled ethanol. This method also resulted in nanomaterials without sufficient charge repulsion for colloidal stability in water,¹² in contrast to the wet-milled nanoPP studied here. Both comparisons highlight how nanomaterial surface properties can be effectively manipulated by the production procedure.

3.5. How do CCM components influence colloidal stability and DLS results?

CCM is a buffered solution (pH 7–7.4) that contains proteins, such as serum albumin or globulins, amino acids, vitamins and salts (typically ~ 150 mM; Table 6). These components influence the balance of attractive and repulsive forces in a dispersion. It is well known that the high electrolyte content in CCM can induce particle aggregation *via* reduction of electrostatic repulsion between two particles with a similar surface charge.⁴⁸ Multivalent electrolytes, such as calcium and magnesium, are more efficient at suppressing charge repulsion than monovalent ions, such as sodium, indicating that both the composition and amount of electrolytes in the CCM influence the morphology and the rate of agglomerate formation.⁴⁹ It is also important to remember that CCM composition can vary based on the metabolic and nutritional needs of different cell types. More importantly, it is different from that of plasma and this may affect the colloidal stability of nanomaterials. Table 6 was reproduced with permission from Moore *et al.* (2015) and compares the composition of the most common CCM, including both the MEM and DMEM-based media employed in the current study. It is interesting to note that DMEM + 10% FBS has both the highest osmolarity



Table 6 Composition and properties of three commonly used CCM, including DMEM + 10% FBS used in this study, compared to human plasma. Modified with permission from Moore *et al.* (2015)

| Component classes and CCM properties | Component/parameter details | DMEM + 10% FBS | MEM + 10% FBS | RPMI + 10% FBS | Human plasma |
|--------------------------------------|--|----------------------------|---------------|----------------|--------------|
| Amino acids | Total (mM) | 10.65 | 5.43 | 6.44 | 2.32–4.05 |
| Vitamins | Total (mM) | 0.15 | 0.04 | 0.24 | <0.07 |
| Cations | Sodium (mM) | 155.31 | 144.44 | 124.27 | 142.00 |
| | Potassium (mM) | 5.33 | 5.33 | 5.33 | 4.00 |
| | Calcium (mM) | 1.80 | 1.80 | 0.42 | 2.50 |
| | Magnesium (mM) | 0.81 | 0.81 | 0.41 | 1.50 |
| | Iron (mM) | 0.25 | 0.25 | n/a | 10–27 |
| | Anions | Chloride (mM) | 117.47 | 124.37 | 100.16 |
| Bicarbonate (mM) | | 44.05 | 26.19 | 23.81 | 27.00 |
| Sulfate (mM) | | 0.81 | 0.81 | 0.41 | 0.50 |
| Nitrate (mM) | | 0.74 | n/a | 0.85 | 20.00 |
| Phosphate (mM) | | 0.92 | 1.01 | 5.63 | 1.00 |
| Proteins | | Total (g L ⁻¹) | 3.00–4.50 | 3.00–4.50 | 3.00–4.50 |
| | Serum albumin (mM) | 0.05 | 0.05 | 0.05 | 0.58 |
| | α -Globulins (g L ⁻¹) | 0.30 | 0.30 | 0.30 | 8.10 |
| | β -Globulins (g L ⁻¹) | 0.27 | 0.27 | 0.27 | 11.50 |
| | γ -Globulins (g L ⁻¹) | 0.07 | 0.07 | 0.07 | 15.60 |
| | IgG (mM) | 3.25 | 3.25 | 3.25 | 0.08 |
| Parameters | pH range | 7.00–7.40 | 7.00–7.40 | 7.00–7.40 | 7.34–7.42 |
| | Osmolality (mOsm kg ⁻¹) | 320–360 | 280–320 | 270–310 | 276–295 |

and content of multivalent ions of the four media listed (including human plasma), which indicates that this medium may be the most destabilizing in terms of charge repulsion reduction and therefore the most challenging in terms of colloidal stability. With the limited dataset provided in this study, samples measured in DMEM *vs.* MEM-based media did not appear to differ substantially in size or PDI. However, further systematic investigations are required to confirm this.

It is important to note that CCM contains a variety of amphiphilic biomolecules, such as proteins, which can adsorb onto the particle surface (thereby changing the surface charge) and achieving colloidal stability primarily *via* steric hindrance with only a minor contribution of charge repulsion.⁹ The important role of steric stabilization is exemplified by the reduction of the zeta potential of most nanomaterials when dispersed in CCM. For example, the ZP of stable dispersions of PS-COOH and nanoPET in CCM were reduced from \sim -42 mV (in MilliQ water) to -11.1 ± 0.8 mV and -10.8 ± 0.5 mV in CCM, respectively. It is important to acknowledge that protein adsorption to the particle surface (*i.e.* biocorona formation) may have opposite effects on colloidal stability, depending upon the material and kind of proteins. In fact, while proteins can improve colloidal stability, in some cases they can promote particle agglomeration (reversible) and aggregation (irreversible). For example, both incomplete surface coverage and particle bridging phenomena (*i.e.* the linkage of two particles *via* the surface coating) can result in agglomeration and aggregation.⁹ Because of these limitations, it is extremely important to validate dispersion SOPs (recommendations in section 3.7) prior to performing routine measurements.^{50,51}

3.6. How did errors in sample handling influence DLS results?

The importance of a well-validated, comprehensive SOP is underlined by the occurrence of errors. One such error in the current study resulted from a change made to the study protocol. In the Langevin *et al.* ILC, the study was conducted with test materials pre-diluted to 1 mg mL⁻¹ in water. In contrast, the current study employed the original concentrated suspensions as starting materials: PS-COOH: 27 or 28 mg mL⁻¹ (depending on lot) and nanoPET: 6 mg mL⁻¹. It was discovered after ILC completion that the difference in starting concentration was not sufficiently highlighted in the modified SOP, leading to handling errors.

3.6.1. The pitfalls of diluting directly into CCM. A single-step dilution of highly concentration PS-COOH directly into CCM resulted in agglomeration (Fig. 6), likely due to a combination of multiple particle–particle interactions at the high concentration, salt-induced reductions to the surface charge and a slower surface coverage with proteins.⁹ In contrast, a two-step dilution, first in water (1 mg mL⁻¹) and then in CCM (0.1 mg mL⁻¹) yielded stable colloidal dispersions (Fig. 6). A single-step dilution of nanoPET (6 mg mL⁻¹) directly into CCM (0.6 mg mL⁻¹) led to variable agglomeration, with Z-Ave values of \sim 40–80 nm larger than the two-step dilution procedure (SI Fig. S5). Based on these observations, we recommend pre-diluting highly concentrated nanoplastics first in water followed by CCM to improve the colloidal stability of the final suspension.

3.6.2. The effect of sample concentration. The effect of varying concentration was also investigated for dilutions in water. It is important to note that Z-Ave values are typically stable across a sample-specific ideal concentration range.²⁷ Below the ideal concentration range, the scattering intensity



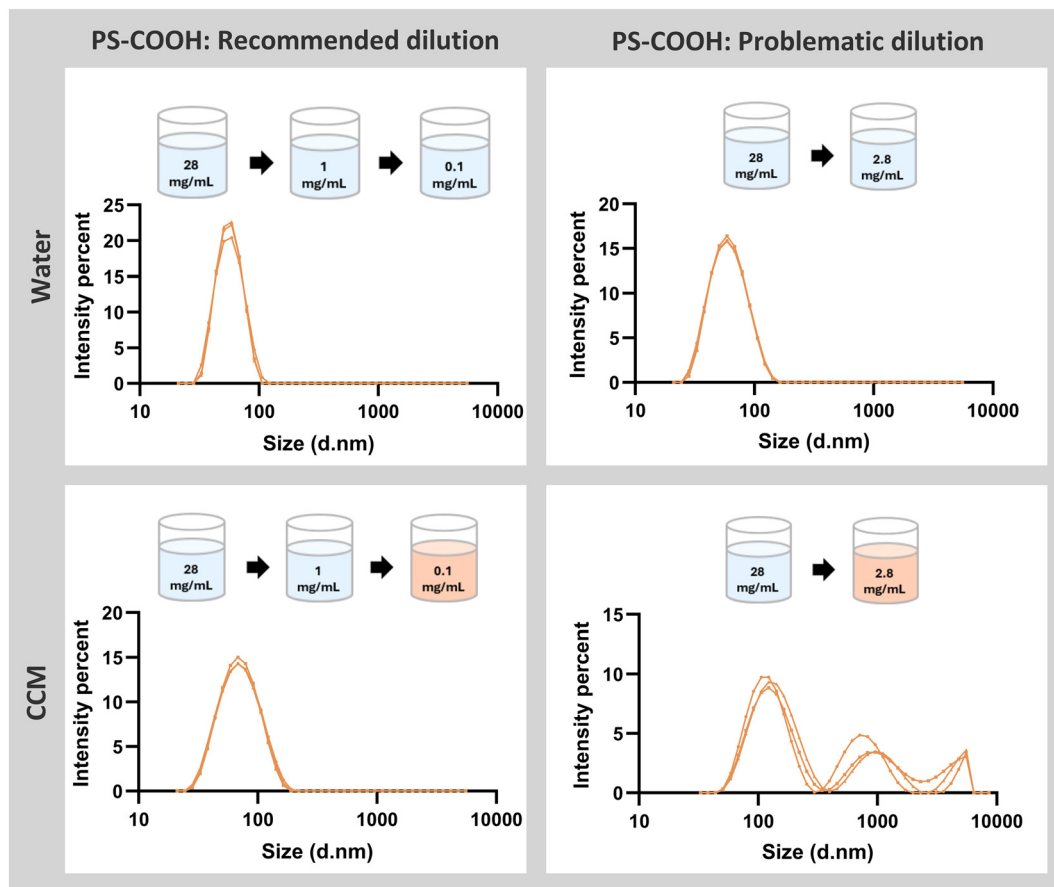


Fig. 6 Hydrodynamic diameter distribution curves of PS-COOH following recommended (left) and problematic (right) dilution procedures in water (top) and CCM (bottom). In the schematic, blue vials represent water as the dispersion medium, while pink vials represent CCM. Three replicate curves are depicted for each procedure.

is too low, resulting in unacceptable signal noise. Above the ideal range, effects such as multiple scattering, restricted diffusion, and particle-particle interactions can occur, which also lead to poor quality measurements and changes to the

measured hydrodynamic diameter.²⁷ Since both the sample scattering potential and the instrument optical configuration can influence these parameters, ISO22412 (2017) guidelines require that the chosen concentration for the DLS

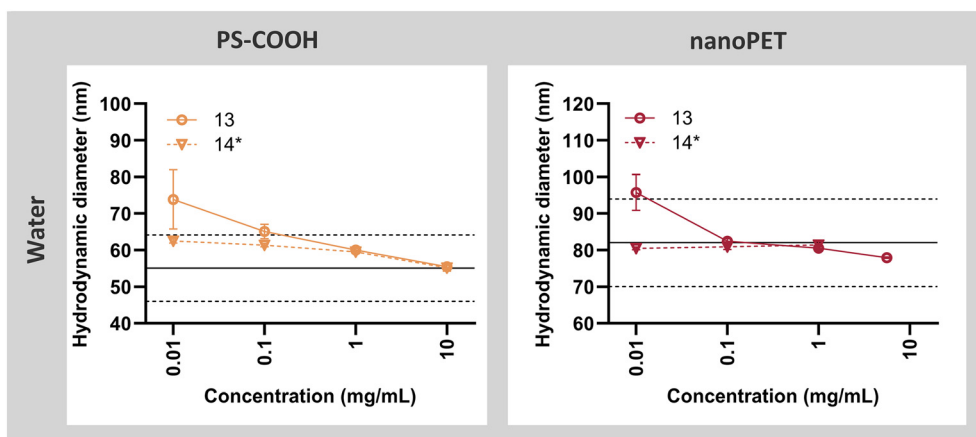


Fig. 7 Scattered light intensity-based harmonic mean hydrodynamic diameter (Z-Ave) of PS-COOH (left) and nanoPET (right) at different concentrations. Black lines depict the weighted global mean x_w , and dashed lines correspond to $\pm 2SD_w$ from Fig. 2 and 3. Values for each measurement depict the $x_i \pm 1SD_i$ ($n = 9$) from one lab with access to a Malvern Panalytic device (13) and an Anton Paar device (14*).



measurement should be within the range where the Z-Ave is stable. This range is typically determined by measuring a series of dilutions and plotting measured size as a function of particle concentration.³²

One laboratory with two instruments (13, 14*) volunteered to measure serial dilutions of PS-COOH and nanoPET in water, comparing the hydrodynamic diameters of the dilutions with the previously established consensus range. Z-Ave values of PS-COOH dilutions were not stable, steadily decreasing with increasing concentration, while the nanoPET Z-Ave values were constant between 0.1–1 mg mL⁻¹ (Fig. 7). Low concentrations (*i.e.*, 0.01 mg mL⁻¹) showed higher variations between measurements and instruments, although it should be noted that only one lab provided these measurements and further replication by other ILC participants is recommended. However, the results suggest that PS-COOH and nanoPET samples measured at elevated concentrations should theoretically fall within the consensus range. For two erroneous PS-COOH samples (2.8 mg mL⁻¹), this was the case (60 ± 1 nm; $n = 18$), while one nanoPET (0.6 mg mL⁻¹) sample fell outside the consensus range (106 ± 1 nm; $n = 9$). Generally, it appears that a measurement concentration of 0.1 mg mL⁻¹ is well-suited for DLS measurements of PS-COOH and nanoPET. DLS measurements of serial dilutions are helpful to establish the ideal measurement range and measurements of moderately higher concentrations are acceptable if within the stable measurement range.

3.7. General recommendations

Since DLS is a technique commonly used by different disciplines involved in plastic research, our aim with this study was to provide practical insights for the wider nanoplastic user community in addition to material developers. Based on the observations from the current study and the literature, we propose three general recommendations (Fig. 8) for the size characterization of nanoplastics using DLS. The first recommendation emphasizes the importance of standardized handling and dilution of nanoplastic test materials, especially when using complex media, such as CCM. To avoid problematic agglomeration or aggregation, a two-step dilution process, first in water and then in complex media, appears to provide good dispersion results. Although exogenous dispersing agents were not needed in this study, some nanoplastics will require such agents to achieve homogenous dispersion.⁵¹ In such cases, a two-step dispersion protocol, first in water containing dispersants, then in CCM has also been shown to achieve similarly good results.¹²

Secondly, we recommend that laboratories routinely measure a benchmark material, such as PS-COOH, using the optimized SOPs published in the ESI. This is useful for checking instrument functionality, ensuring that all settings are correct, training new users and adding useful benchmark data to the literature. When evaluating new test materials, we

| Recommendations | |
|-----------------|---|
| DILUTE | <ol style="list-style-type: none"> 1. Dilute highly concentrated dispersions to 1 mg/mL with water 2. Then dilute with CCM to 0.1 mg/mL |
| BENCH-MARK | <ol style="list-style-type: none"> 1. Measure your sample and benchmark material in water 2. CV < 10% is acceptable for dispersions in water |
| VERIFY | <ol style="list-style-type: none"> 1. Measure more often in CCM (the variability will be higher). 2. CV < 30% is acceptable for dispersions in CCM |

Fig. 8 Recommendations for DLS size measurements of nanoplastics in water and CCM.

encourage labs to produce multiple replicate datasets in water before moving on to measurements in CCM. Size data generated in water provides a valuable reference for the more variable size data generated in complex media. Furthermore, it should be highlighted that the nanoPET and nanoPP materials studied here, despite their increasing complexity, are still “model” nanoplastics and not true environmental particles. Naturally weathered nanoplastics will likely exhibit an even greater complexity, such as a broader size distribution, high sample-to-sample variability, different surface modifications and eco-coronas. Therefore, understanding the sources of data variation in DLS measurements and the use of complementary sizing techniques (such as image-based analysis) is important for understanding complex environmental samples.

To further improve comparisons of DLS measurement quality across users and test materials, we recommend documentation and reporting of CV_w values whenever possible. As a general guide, CV values of DLS measurements in water should not exceed 10%. This arbitrary limit, based on empirical data from the current study and literature, appears to be suitable for both spherical, monodisperse samples (*e.g.* PS-COOH) as well as irregular shaped samples with a greater polydispersity (*e.g.* nanoPET and nanoPP). Due to the greater inherent degree of measurement variability observed for dispersions in CCM,^{9,26} we recommend a CV of <30% as a realistic guide for tolerable measurement variability of nanoplastics dispersed in CCM. Importantly, it should be emphasized that the proposed CV thresholds (<10% in water, <30% in CCM) are valuable guidance criteria but should not be misinterpreted as universal standards, since they are derived from empirical observations



reported in two limited datasets and are not regulatory specifications. We therefore caution against over interpretation of these values.

4. Conclusions

In contrast to previously published ILCs for DLS measurements, which used narrowly dispersed, spherical test materials, this study investigated a series of nanoplastics with increasing complexity in terms of particle shape and polydispersity (PS-COOH, nanoPET and nanoPP). Based on the greater complexity of the nanoPET and nanoPP materials, it was expected that the measurement variability between labs (expressed both by the consensus range and the CV) would be larger for nanoPET and nanoPP, when measured in water. Contrary to expectations, the nanoPET and nanoPP showed lower CV values (7.3 and 6.8%; respectively) than PS-COOH (8.2%). The data also indicate that the shape factor and moderate sample polydispersity do not contribute strongly to inter-laboratory variation. Instead, sample handling and dispersion in complex media, such as CCM, appeared to be the causes of greater measurement variability, which has been previously reported. For samples diluted in CCM, the CV increased to 15.9% (PS-COOH) and 14.2% (nanoPET), which is lower than literature reports. CV values of <10% and 30% in water and CCM, respectively, are useful quality metrics for DLS measurements of nanoplastics. Most importantly, careful construction of SOPs and strict adherence to these are required to reduce measurement variability in both water and complex media.

Author contributions

K. Altmann: conceptualization, funding acquisition, supervision, resources, writing – review & editing; R. Portela: conceptualization, funding acquisition, supervision, resources, writing – review & editing, F. Barbero: conceptualization, funding acquisition, supervision, resources, writing – review & editing, E. Breuninger: investigation, formal analysis, validation; L. M. A. Camassa: investigation, T. Cirkovic Velickovic: conceptualization, funding acquisition, supervision, resources, writing – review & editing, C. Charitidis: investigation, A. Costa: data curation; supervision; writing – review & editing, M. Fadda: investigation, formal analysis, writing – review & editing; P. Fengler: investigation, I. Fenoglio: data curation; supervision; writing – review & editing, A. M. Giovannozzi: investigation, Ø. Haugen: investigation, data curation; supervision; writing – review & editing, P. Kainourgios: investigation, F. von der Kammer: curation; supervision; writing – review & editing, M. J. Kirchner: investigation, formal analysis, validation, writing – review & editing; M. Lomax-Vogt: investigation, formal analysis, validation; T. Lujic: investigation, F. Milczewski: investigation, M. A. Moussawi: investigation, Simona Ortelli: investigation, T. Parac-Vogt: data curation; supervision; A.

Potthoff: conceptualization, funding acquisition, supervision, resources, writing – review & editing, J. J. Reinos: investigation, S. Röscher: investigation, A. Sacco: investigation, Lukas Wimmer: investigation, writing – review & editing, I. Zaroni: investigation, methodology, writing – review & editing; L. A. Dailey: conceptualization, funding acquisition, supervision, resources, writing – original draft preparation.

Conflicts of interest

There are no conflicts of interest to declare.

Data availability

Data for this article, including standard operating procedures, spreadsheets of all particle size distribution data and correlograms is published on Zenodo: <https://doi.org/10.5281/zenodo.17105630>.

Supplementary information is available. See DOI: <https://doi.org/10.1039/d5en00645g>.

Acknowledgements

The authors thank the European commission for funding from the European Union's Horizon 2020 research and innovation program under grant agreement #964766 (POLYRISK), #965367 (PlasticsFate), and #965173 (Imptox). All projects are part of the European cluster to understand the health impacts of micro- and nanoplastics (CUSP). The authors thank the project 21GRD07 PlasticTrace (Funder ID: 10.13039/100019599) which has received funding from the European Partnership on Metrology, co-financed from the European Union's Horizon Europe Research and Innovation Programme and by the Participating States". The authors thank Dmitri Ciornii for SEM measurements. We are also very grateful to Anil Patri, Goutam Palui, and Kaylee Solano of the United States Food and Drug Administration for their DLS measurements and fruitful discussions.

References

- 1 International Organization for Standardization, 2020.
- 2 European Commission, 2023.
- 3 L. M. Hernandez, N. Yousefi and N. Tufenkji, *Environ. Sci. Technol. Lett.*, 2017, **4**, 280–285.
- 4 W. Zhang, Z. Dong, L. Zhu, Y. Hou and Y. Qiu, *ACS Nano*, 2020, **14**, 7920–7926.
- 5 L. M. Hernandez, E. G. Xu, H. C. E. Larsson, R. Tahara, V. B. Maisuria and N. Tufenkji, *Environ. Sci. Technol.*, 2019, **53**, 12300–12310.
- 6 J. Hildebrandt and A. F. Thünemann, *Macromol. Rapid Commun.*, 2023, **44**(6), 2200874.
- 7 J. R. Peller, S. P. Mezyk, S. Shidler, J. Castleman, S. Kaiser, R. F. Faulkner, C. D. Pilgrim, A. Wilson, S. Martens and G. P. Horne, *Environ. Pollut.*, 2022, **313**, 120171.



- 8 J. Seghers, E. A. Stefaniak, R. La Spina, C. Cella, D. Mehn, D. Gilliland, A. Held, U. Jacobsson and H. Emteborg, *Anal. Bioanal. Chem.*, 2022, **414**, 385–397.
- 9 T. L. Moore, L. Rodriguez-Lorenzo, V. Hirsch, S. Balog, D. Urban, C. Jud, B. Rothen-Rutishauser, M. Lattuada and A. Petri-Fink, *Chem. Soc. Rev.*, 2015, **44**, 6287–6305.
- 10 M. Das, L. Calderon, D. Singh, S. Majumder, L. Bazina, N. Vaze, U. Trivanovic, G. DeLoid, N. Zuverza-Mena, M. Kaur, J. Konkol, N. K. Tittikpina, G. Tsilomelekis, O. Sadik, J. C. White and P. Demokritou, *NanoImpact*, 2025, **38**, 100567.
- 11 K. Altmann, L. Wimmer, V. Alcolea-Rodriguez, T. Waniek, V. Wachtendorf, K. Matzdorf, D. Ciornii, P. Fengler, F. Milczewski, I. Otazo-Aseguinolaza, M. Ferrer, M. A. Bañares, R. Portela and L. A. Dailey, *J. Hazard. Mater.*, 2025, **497**, 139595.
- 12 L. Wimmer, M. V. N. Hoang, J. Schwarzingler, V. Jovanovic, B. Andelković, T. C. Velickovic, T. C. Meisel, T. Waniek, C. Weimann, K. Altmann and L. A. Dailey, *Environ. Sci.: Nano*, 2025, **12**, 2667–2686.
- 13 International Organization for Standardization, 2024.
- 14 International Organization for Standardization, 2015.
- 15 International Organization for Standardization, 2017.
- 16 National Institute of Standards and Technology.
- 17 G. Crosset-Perrotin, A. Moraz, R. Portela, V. Alcolea-Rodriguez, D. Burrueco-Subirà, C. Smith, M. A. Bañares, H. Foroutan and D. H. Fairbrother, *Environ. Sci.: Nano*, 2025, **12**, 2911–2964.
- 18 P. Merdy, F. Delpy, A. Bonneau, S. Villain, L. Iordachescu, J. Vollertsen and Y. Lucas, *Heliyon*, 2023, **9**(8), 18387.
- 19 K. Y. Santizo, H. S. Mangold, Z. Mirzaei, H. Park, R. R. Kolan, G. Sarau, S. Kolle, T. Hansen, S. Christiansen and W. Wohlleben, *Small*, 2025, **21**, 2405555.
- 20 F. Caputo, R. Vogel, J. Savage, G. Vella, A. Law, G. Della Camera, G. Hannon, B. Peacock, D. Mehn, J. Ponti, O. Geiss, D. Aubert, A. Prina-Mello and L. Calzolari, *J. Colloid Interface Sci.*, 2021, **588**, 401–417.
- 21 H. Kato, M. Suzuki, K. Fujita, M. Horie, S. Endoh, Y. Yoshida, H. Iwahashi, K. Takahashi, A. Nakamura and S. Kinugasa, *Toxicol. In Vitro*, 2009, **23**, 927–934.
- 22 A. Marucco, E. Aldieri, R. Leinardi, E. Bergamaschi, C. Riganti and I. Fenoglio, *Materials*, 2019, **12**(23), 3833.
- 23 C. Ompala, J.-P. Renault, O. Taché, É. Cournède, S. Devineau and C. Chivas-Joly, *J. Hazard. Mater.*, 2024, **469**, 134083.
- 24 I. Zanoni, L. Briccolani, L. Faccani, M. Blosi, S. Ortelli, M. Crosera, G. Marussi, S. Albonetti and A. L. Costa, *Environ. Sci. Eur.*, 2025, **37**, 21.
- 25 R. T. Coones, C. Minelli and V. Kestens, *J. Nanopart. Res.*, 2025, **27**, 170.
- 26 D. Langevin, O. Lozano, A. Salvati, V. Kestens, M. Monopoli, E. Raspaud, S. Mariot, A. Salonen, S. Thomas, M. Driessen, A. Haase, I. Nelissen, N. Smisdom, P. P. Pompa, G. Maiorano, V. Puntès, D. Puchowicz, M. Stępnik, G. Suárez, M. Riediker, F. Benetti, I. Mičetić, M. Venturini, W. G. Kreyling, M. van der Zande, H. Bouwmeester, S. Milani, J. O. Rädler, S. Mülhopt, I. Lynch and K. Dawson, *NanoImpact*, 2018, **10**, 97–107.
- 27 K. Takahashi, J. A. Kramar, N. Farkas, K. Takahata, I. Misumi, K. Sugawara, S. Gonda and K. Ehara, *Metrologia*, 2019, **56**, 055002.
- 28 K. Takahashi, 2025.
- 29 A. Robles-Martín, R. Amigot-Sánchez, L. Fernandez-Lopez, J. L. Gonzalez-Alfonso, S. Roda, V. Alcolea-Rodriguez, D. Heras-Márquez, D. Almendral, C. Coscolín, F. J. Plou, R. Portela, M. A. Bañares, Á. Martínez-del-Pozo, S. García-Linares, M. Ferrer and V. Guallar, *Nat. Catal.*, 2023, **6**, 1174–1185.
- 30 H. Bresch, V.-D. Hodoroaba, A. Schmidt, K. Rasmussen and H. Rauscher, *Nanomaterials*, 2022, **12**(13), 2238.
- 31 X. Zhang, J. Qiu, X. Li, J. Zhao and L. Liu, *Appl. Opt.*, 2020, **59**, 2337–2344.
- 32 International Organization for Standardization, 2017.
- 33 D. E. Koppel, *J. Chem. Phys.*, 1972, **57**, 4814–4820.
- 34 Malvern Panalytical.
- 35 International Organization for Standards, 2023.
- 36 U. Nobbmann, 2017, <https://www.malvernpanalytical.com/en/learn/knowledge-center/insights/polydispersity-what-does-it-mean-for-dls-and-chromatography>. Accessed 10 July 2025.
- 37 S. Balog, L. Rodriguez-Lorenzo, C. A. Monnier, M. Obiols-Rabasa, B. Rothen-Rutishauser, P. Schurtenberger and A. Petri-Fink, *Nanoscale*, 2015, **7**, 5991–5997.
- 38 T. L. Doane, C.-H. Chuang, R. J. Hill and C. Burda, *Acc. Chem. Res.*, 2012, **45**, 317–326.
- 39 J. Lyklema, *Fundamentals of interface and colloid science. Volume 2: Solid-liquid interfaces*, Academic Press, London, 1995.
- 40 D. V. Matyushov, *Mol. Phys.*, 2014, **112**, 2029–2039.
- 41 M. K. Rasmussen, J. N. Pedersen and R. Marie, *Nat. Commun.*, 2020, **11**, 2337.
- 42 R. Yan, S. Lin, W. Jiang, X. Yu, L. Zhang, W. Zhao and Q. Sui, *Sci. Total Environ.*, 2023, **898**, 165431.
- 43 K. C. Jena, R. Scheu and S. Roke, *Angew. Chem., Int. Ed.*, 2012, **51**, 12938–12940.
- 44 X. Yan, M. Delgado, J. Aubry, O. Gribelin, A. Stocco, F. Boisson-Da Cruz, J. Bernard and F. Ganachaud, *J. Phys. Chem. Lett.*, 2018, **9**, 96–103.
- 45 R. Vácha, O. Marsalek, A. P. Willard, D. J. Bonthuis, R. R. Netz and P. Jungwirth, *J. Phys. Chem. Lett.*, 2012, **3**, 107–111.
- 46 Y. Uematsu, D. J. Bonthuis and R. R. Netz, *Langmuir*, 2020, **36**, 3645–3658.
- 47 Y. Uematsu, D. J. Bonthuis and R. R. Netz, *Curr. Opin. Electrochem.*, 2019, **13**, 166–173.
- 48 L. H. Allen and E. Matijević, *J. Colloid Interface Sci.*, 1969, **31**, 287–296.
- 49 R. A. French, A. R. Jacobson, B. Kim, S. L. Isley, R. L. Penn and P. C. Baveye, *Environ. Sci. Technol.*, 2009, **43**, 1354–1359.
- 50 D. Lizonova, U. Trivanovic, P. Demokritou and G. A. Kelesidis, *Nanomaterials*, 2024, **14**(7), 589.
- 51 D. van Uunen, M. Kloukinioti, I. M. Kooter, E. M. Höppener, L. E. A. Yoe, A. M. Brunner, A. Boersma and L. A. Parker, *Environ. Pollut.*, 2024, **356**, 124306.

